Coincident Fragment Detection in Strong Field Photoionization and Dissociation of H_2

H. Rottke, C. Trump, M. Wittmann, G. Korn, and W. Sandner
Max-Born-Institut, Max-Born-Strasse 2a, D-12489 Berlin, Germany

R. Moshammer,[1] A. Dorn,[1] C. D. Schröter,[1] D. Fischer,[1] J. R. Crespo Lopez-Urrutia,[1]
P. Neumayer,[1,2] J. Deipenwisch,[1] C. Höhr,[1] B. Feuerstein,[1] and J. Ullrich[1]
[1]*Max-Planck-Institut für Kernphysik, Saupfercheckweg 1, D-69117 Heidelberg, Germany*
[2]*Gesellschaft für Schwerionenforschung mbH Planckstrasse 1, D-64291 Darmstadt, Germany*
(Received 29 May 2001; published 14 June 2002)

Electron-ion momentum spectroscopy is used to investigate the correlated electronic and nuclear motion in fragmentation of H_2 in 4×10^{14} W/cm^2, 25 fs laser pulses at 795 nm. Reaction channel dependent photoelectron spectra indicate that besides the main, stepwise H_2 ionization H_2^+ dissociation mechanism resulting in the products $H(1s) + H^+ + e^-$ a second new mechanism has to be assumed. The momentum distribution of H^+ ions in the dissociation channels $H(1s) + H^+ + e^-$ and $2H^+ + 2e^-$ is found to be independent of the kinetic energy of the photoelectrons.

DOI: 10.1103/PhysRevLett.89.013001 PACS numbers: 33.80.Rv, 33.80.Wz

Since the first experimental investigation on molecular hydrogen exposed to high intensity light pulses [1], a series of experiments concentrated on the analysis and interpretation of either photoelectron spectra or the angle resolved kinetic energy distribution of charged H^+ photodissociation products. Similar to atoms, photoelectron distributions showed above threshold ionization (ATI) and resonance structures, induced by ac-Stark shifting molecular energy levels [2] which enhance multiphoton ionization [3]. Besides simple photoionization with the formation of H_2^+, charged dissociation products H^+ were always found [1,4–7], demonstrating that photoelectrons emerge from different excitation pathways of the molecule. It is commonly accepted that dissociation starts after photoionization of the neutral molecule. Dissociation pathways are effective one- and two-photon dissociation, also known as bond softening and above threshold dissociation [1] (mechanisms introduced by [8,9]), and Coulomb explosion occurring after removal of the second electron from the molecule [4]. The existence of Coulomb explosion was confirmed by Frasinski *et al.* in an experiment where correlation among photoions was investigated [4] using covariance mapping [10]. With the same technique it was tried to explore electron-ion and electron-electron correlation [4].

In order to selectively record photoelectron spectra for different dissociation channels, to reveal the interplay between electronic and nuclear motion for the various H_2 fragmentation pathways, and to identify possible electron-electron correlation in the Coulomb explosion channel, we performed a kinematically complete experiment. The vector momenta of all charged fragments emerging from single ionization/dissociation events were measured in coincidence for a large part of the final state momentum space, i.e., for all relevant energy sharings and relative emission angles of all emerging fragments. In this Letter we present a partial kinematical analysis for the reaction channels:

$$H_2 \rightarrow H_2^+ + e^-, \tag{1}$$

$$H_2 \rightarrow H^+ + H + e^-, \tag{2}$$

$$H_2 \rightarrow H^+ + H^+ + e^- + e^-. \tag{3}$$

For all three channels electron spectra are measured, and the dependence of the H^+ ion momenta on the kinetic energy of the photoelectrons is investigated for reactions (2) and (3). Surprisingly, the electron kinetic energy distributions for channels (1) and (2) differ significantly, leading to the conclusion that besides the main, well accepted, stepwise H_2 ionization/dissociation mechanism a second mechanism has to be active.

Our experimental setup was based on cold target recoil ion momentum spectroscopy (COLTRIMS) [11]. It was identical to the one we used to investigate strong field nonsequential atomic photoionization [12], now completed with a combined time-of-flight multelectron spectrometer to form a "reaction microscope" [11]. A homogeneous magnetic field ($B = 4.9 \times 10^{-4}$ T), parallel to an electric field ($E = 2$ V/cm) for ion and electron extraction, was applied over the electron drift tube to guide electrons with large momentum component $\vec{p}_\perp$ perpendicular to the spectrometer axis to the electron detector. Electrons were first accelerated over a path of 10 cm, then passed a 10 cm field free drift tube until they finally hit a multichannel plate detector equipped with a position sensitive multihit delay-line anode. With this setup it was possible to detect all photoelectrons with $|\vec{p}_\perp| \leq 0.8$ a.u. and momenta parallel to the spectrometer axis $p_{||} \geq -1.1$ a.u. (electrons and ions are assigned a positive $p_{||}$ if initially they were emitted into the direction where the e^- detector was mounted). H^+ ions hitting the ion detector have a maximum momentum perpendicular to the spectrometer axis $|\vec{p}_\perp| = 3$ a.u. if

$p_{||} < 0$ and $|\vec{p}_{\perp}| = 2.3$ a.u. if $p_{||} > 0$. All H_2^+ ions were detected, irrespective of the momentum they gain in the H_2 photoionization step. From the measured positions and times of flight the complete momentum vector for any individual electron and ion is obtained [11]. Detecting electrons and ions simultaneously over a large part of the final momentum space allowed us to perform a complete kinematical analysis of the breakup of molecular hydrogen into charged fragments.

Care was taken to have less than one breakup reaction in each laser shot on the average in order to ensure that fragments emerge from a single molecule. The momentum spectrometers were therefore mounted in an ultrahigh vacuum chamber with a base pressure of less than 5×10^{-11} mbar. Hydrogen was admitted as a supersonic molecular beam [12] with a density in the focal spot of the light beam of about 10^8 molecules/cm^3.

The hydrogen molecules were excited by pulsed Ti:sapphire laser radiation intersecting the molecular beam at right angle. The light pulses with 795 nm center wavelength and 25 fs pulse width were generated by a Kerr-lens mode locked oscillator and amplified to pulse energies of up to 600 μJ at 1 kHz repetition rate. The beam was focused with an on-axis spherical mirror ($f = 100$ mm) to a spot size with 8 μm in diameter (FWHM). The light intensity in the focal spot was set to 4×10^{14} W/cm^2 and the width of the molecular beam sheet along the light beam axis to $\approx$50 μm. The spatial intensity variation along the light beam axis within the molecular beam is estimated to be at most 10% of the maximum intensity.

Figure 1 shows the photoelectron kinetic energy distributions in the reaction channels (1), (2), and (3). Electrons emitted into a range of polar angles θ between 0 and 25° with respect to the direction of polarization of the light beam, towards the electron detector are included. For reaction channel (1) all electrons found together with an H_2^+ ion are taken into account, without any further restriction on the H_2^+ momentum. Only conservation of the total momentum restricts the accepted events to ions with a momentum opposite to that of the corresponding electron. For channels (2) and (3) the events included in the spectra are further restricted by the geometric angle of acceptance for H^+ ions (see above). The coincidence criterion is the detection of at least one H^+ ion. The spectrum shown for reaction (2) encompasses the H_2^+ dissociation channels known as effective one- and two-photon dissociation for excitation near 795 nm ([7] and references cited therein). In the channel (3) spectrum (Coulomb explosion) all events are included where one or two electrons were detected after double ionization of H_2. In case of two electrons only the kinetic energy of the electron arriving first at the detector is plotted. The spectra were recorded at a light intensity of 4×10^{14} W/cm^2. The energy bin size is 150 meV [channel (1)] and 300 meV [channels (2),(3)], respectively. To reveal the overall properties of the kinetic energy distributions, the number of events per energy bin is displayed

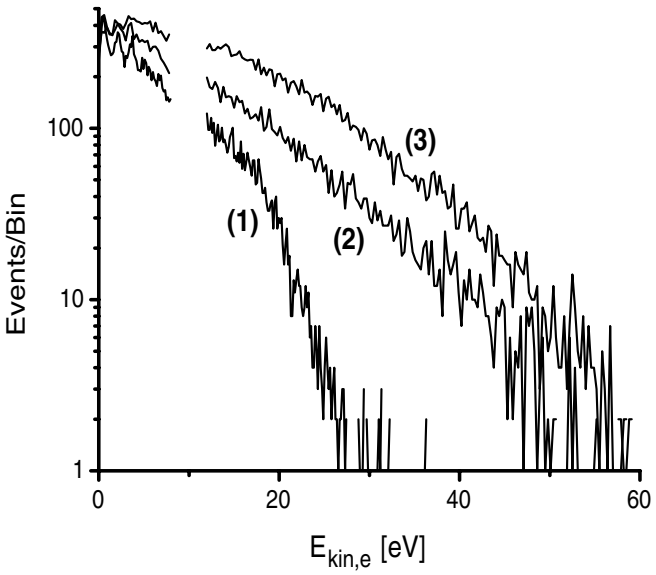

FIG. 1. Reaction channel selective electron kinetic energy distributions for reactions (1), (2), and (3). Only events with the electron emitted into a cone with acute angle 25° along the light polarization vector are included. The light pulse intensity was 4×10^{14} W/cm^2.

on a logarithmic scale. Missing data points between 8 and 12 eV correspond to an electron time of flight where the transverse momentum resolution drops to zero due to the cyclotron motion in the applied magnetic field.

At low electron kinetic energies we find a pronounced ATI structure in channel (1). Remnants of such a structure are also found in the two dissociation channels (2) and (3). In Fig. 1 they are barely visible due to the large energy bin size chosen in order to display the high energy part of these spectra.

On the average (disregarding the low energy ATI structure) the simple photoionization spectrum of H_2 [reaction (1)] shows a characteristic dependence on the electron kinetic energy. On a logarithmic scale the electron yield decreases approximately linearly with increasing $E_{\mathrm{kin},e}$ with an abrupt increase in the slope at $E_{\mathrm{kin},e} = 18$ eV. Beyond $E_{\mathrm{kin},e} = 28$ eV practically no electrons were detected. This "cutoff" may be understood by considering the light intensity I_{sat} where ionization of H_2 saturates in a 25 fsec light pulse. From measurements of Thompson *et al.* [7] I_{sat} is calculated to be approximately 2.5×10^{14} W/cm^2. This is significantly lower than the intensity I_{max} used. Neutral H_2 molecules do not experience intensity levels in the light pulses beyond I_{sat}. Thus, I_{sat}, and not I_{max}, determines the highest drift energy photoelectrons from reaction (1) may gain by acceleration in the light pulse. For the bulk of electrons which directly leave the molecule without rescattering on the ion core the highest final energy accessible is $E_{\mathrm{kin},e} = 2U_p(I_{\mathrm{sat}}) = E_{\mathrm{sat}}^2/2\omega^2$ (with E_{sat} the electric field strength of the light wave at saturation). This estimate relies on the realistic assumption that electrons enter the

ionization continuum with a kinetic energy which is small compared to the energy gain by subsequent acceleration. At the H_2 saturation intensity $2U_p = 30$ eV. This is in good agreement with the observed cutoff of the H_2 photoionization spectrum [(1) in Fig. 1]. Elastic rescattering of the electron on the H_2^+ ion core may give rise to electrons with a kinetic energy higher than $2U_p$ [13]. Detecting no electrons in this energy range means that the probability of rescattering without destroying the H_2^+ ion is at least 3 orders of magnitude smaller than for direct electron ejection.

In the Coulomb explosion channel (3) and surprisingly also in the dissociation channel (2) the electron kinetic energy distributions show a completely different behavior (Fig. 1). The most prominent difference is found for electron kinetic energies higher than $2U_p(I_{\mathrm{sat}})$. A significant amount of electrons appears here in the dissociation channel. In this energy range the electron kinetic energy distribution looks very similar to the spectrum in channel (3). One would have expected a photoelectron spectrum similar to that of reaction (1); i.e., the spectrum in the dissociation channel should also terminate near $2U_p(I_{\mathrm{sat}})$ if ionization of H_2 strictly precedes dissociation of the molecule by the proposed mechanisms effective one- and two-photon dissociation of H_2^+ ([7] and references cited therein). Contrary, it extends out to $\approx$50 eV which corresponds approximately to $2U_p(I_{\mathrm{max}}) = 50$ eV with I_{max} being the light pulse peak intensity. Even if dissociating H_2^+ states are assumed to be populated efficiently at a somewhat higher intensity level in the light pulse, H_2 depopulation at the saturation intensity for ionization should terminate the electron kinetic energy distribution in the dissociation channel also close to $2U_p(I_{\mathrm{sat}})$.

What is the mechanism that allows the photoelectron to gain significantly more energy in reaction (2) than in (1)? We will discuss two possibilities: (1) ionization and dissociation are strictly sequential, and (2) the electron becomes excited into a bound state and stays near the H_2^+ ion core while dissociation of the excited complex already proceeds. Electric field ionization is appropriate to describe the H_2 ionization step near the H_2 equilibrium internuclear separation. The final kinetic energy of the electron is thus mainly determined by the drift energy it acquires. This in turn depends on the phase of the oscillating electric field when it becomes free with small initial momentum. For strictly sequential ionization/dissociation rescattering has to be assumed for an electron to reach $E_{\mathrm{kin},e} > 30$ eV. After elastic or inelastic scattering on its parent ion core, it may gain an energy which is significantly higher than $2U_p(I_{\mathrm{sat}})$ by acceleration in the light pulse [up to $\approx 10U_p(I_{\mathrm{sat}})$ [13]]. Two kinds of rescattering scenarios may be responsible for the fast photoelectrons. Inelastic scattering with vibrational excitation of the H_2^+ ion into states dissociating in the light pulse may happen. As is known from experiments H_2^+ ions are created in vibrational levels $v = 0, 1$ in the H_2 photoionization step [14]. They are difficult to dissociate and would be good candidates for this mechanism. Assuming this mechanism means that it should have a probability at least 1 order of magnitude higher than rescattering without dissociation of H_2^+, as can be seen from the electron spectra [channels (1) and (2)]. Besides this mechanism, an enhanced elastic scattering probability for dissociating ions may be envisaged. After the electron enters the ionization continuum it gets accelerated and then returns to the ion core within the span of time of one oscillation period ($T = 2.6$ fsec) of the light wave. Meanwhile the internuclear separation R increases, especially fast for already dissociating ions, starting near the H_2 equilibrium internuclear separation ($R = 1.4$ a.u. [15]) where H_2^+ is formed in a vertical transition by ionization of H_2. This increase in R may give rise to an enhanced scattering cross section and therefore an enhanced yield of fast electrons in reaction (2) compared to simple ionization [channel (1)].

The enhanced $e - H_2^+$ scattering cross sections which have to be assumed may be questionable. They are not needed for a mechanism based on delayed ionization of H_2. In a first step the electron gets excited to a bound state. From atoms it is known that excited Rydberg states with a not too low principal quantum number are stable against strong field photoionization [16]. Like the H_2^+ ion, H_2 Rydberg molecules may dissociate in the strong light pulse. Experiments at 526 nm excitation wavelength indicated that dissociating H_2 Rydberg states become populated by strong field excitation [17]. The dissociation mechanism is the same as for the ion, a strong, at a certain internuclear separation (here $R \approx 4.5$ a.u.) resonant, dipole coupling between the $1s\sigma_g$ and $2p\sigma_u$ H_2 core electron states. The coupling induces a core electron charge oscillation between the nuclei and therefore a strong dipole moment oscillating in time. It reaches $\approx$2 a.u. at $R \approx 4.5$ a.u. [18]. The oscillating dipole may kick off the Rydberg electron with high probability compared with the small ionization probability through direct interaction of the Rydberg electron with the light pulse. This ionization mechanism should be most effective for dissociating molecules which reach and even pass the internuclear separation with strong resonant charge oscillation. The time elapsing between excitation of the electron to the Rydberg state at the H_2 equilibrium internuclear separation and the internuclear separation reaching the critical value is long enough for the intensity level in the light pulse to rise significantly into the regime higher than the saturation intensity for H_2 ionization. Ionization of the Rydberg electron then directly results in a drift energy of the photoelectron beyond $2U_p(I_{\mathrm{sat}})$ without the necessity to assume further rescattering.

This mechanism is supported by the electron kinetic energy distribution in the Coulomb explosion channel (Fig. 1). To the right of the cutoff energy for simple ionization [28 eV, channel (1)] the distribution functions for reaction channels (2) and (3) show a very similar

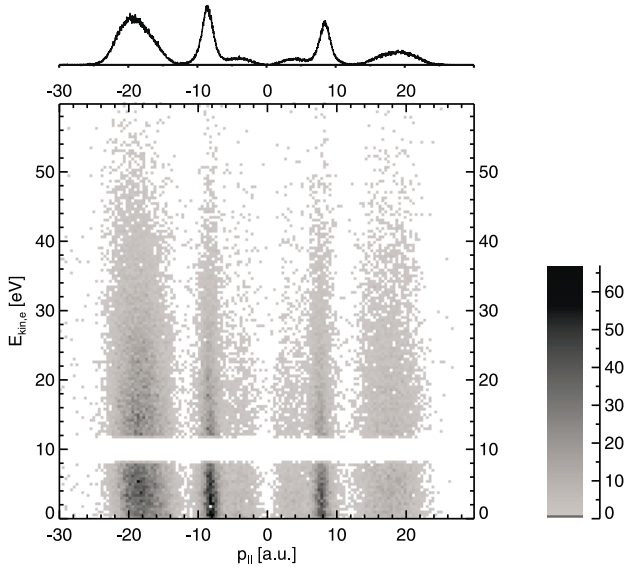

FIG. 2. Correlation plot of the electron kinetic energy $E_{\mathrm{kin},e}$ versus the H^+ ion momentum $p_{||}$ measured in coincidence for the reactions (2) and (3). The experimental conditions are the same as in Fig. 1. On top the integral H^+ momentum distribution is shown.

dependence on the kinetic energy. Ionization of $H_2{}^+$ which results in Coulomb explosion preferentially also occurs near the internuclear separation where the electron charge oscillation is strong [19]. It therefore happens at similar intensity levels creating electrons with similarly high drift energy.

The electron kinetic energy distributions (Fig. 1) have been extracted from Fig. 2. For the dissociation channels (2) and (3) it shows the number of events sorted according to the kinetic energy of the photoelectron ($E_{\mathrm{kin},e}$) and the momentum parallel to the light polarization direction of the H^+ ion ($p_{||}$) detected in coincidence with the electron. The solid angle of emission of the electron is the same as in Fig. 1. Events from H_2 double ionization and subsequent Coulomb explosion [channel (3)] are found in the ion momentum intervals $[-25$ a.u., -12 a.u.] and [12 a.u., 25 a.u.]. $H_2{}^+$ dissociation [channel (2)] contributes in the interval $[-12$ a.u., 12 a.u.]. As in Fig. 1, the horizontal gap in Fig. 2 is the energy range where the electron energy resolution drops to zero.

The measured distribution function clearly shows that the H^+ momentum distribution does not depend significantly on the kinetic energy of the photoelectron for channel (2), as well as for channel (3). The final kinetic energy of the electron is a measure of the light intensity $I(t_0)$ at the time t_0 when it enters the ionization continuum via the relation $E_{\mathrm{kin},e} = U_p[I(t_0)](1 - \cos 2\omega t_0)$. Here it is assumed that the initial electron momentum can be neglected compared to its drift momentum and it does not rescatter. Thus, a certain energy can be reached only if the instantaneous intensity in the light pulse $I(t_0)$ is high enough. The spectrum in Fig. 2 therefore indicates that the ion momentum distribution is insensitive to the intensity level in the light pulse where H_2 is photoionized dissociation starts and double ionization of H_2 initiates Coulomb explosion.

In conclusion, the simultaneous measurement of ion and electron momenta for single strong field H_2 fragmentation events allowed the measurement of fragmentation channel selective electron kinetic energy distributions and of the correlation function for the electron kinetic energy and the momentum of H^+ ions formed in coincidence in reactions (2) and (3). The channel selective electron energy distributions indicate that a new H_2 ionization mechanism has to be assumed to interpret the differences found in the fragmentation channels (1) and (2). This mechanism has to be able to account for the fast electrons in reaction (2). It is certainly active together with stepwise sequential ionization/dissociation of H_2. The relative importance of both mechanisms at low electron energies cannot be judged from the data. The results show that COLTRIMS is capable of allowing a complete kinematical analysis of strong field molecular processes.

[1] A. Zavriyev *et al.,* Phys. Rev. A **42**, 5500 (1990).
[2] R. R. Freeman *et al.,* Phys. Rev. Lett. **59**, 1092 (1987).
[3] H. Rottke, J. Ludwig, and W. Sandner, Phys. Rev. A **54**, 2224 (1996).
[4] L. J. Frasinski *et al.,* Phys. Rev. A **46**, R6789 (1992).
[5] G. N. Gibson *et al.,* Phys. Rev. Lett. **79**, 2022 (1997).
[6] T. D. G. Walsh, F. A. Ilkov, and S. L. Chin, J. Phys. B, At. Mol. Opt. Phys. **30**, 2167 (1997).
[7] M. R. Thompson *et al.,* J. Phys. B, At. Mol. Opt. Phys. **30**, 5755 (1997).
[8] A. I. Pegarkov and L. P. Rapoport, Opt. Spektrosk. **63**, 501 (1987); [Opt. Spectrosc. **63**, 293 (1987)] A. I. Pegarkov and L. P. Rapoport, Opt. Spektrosk. **63**, 751 (1987) [Opt. Spectrosc. **63**, 444 (1987)].
[9] A. Giusti-Suzor *et al.,* Phys. Rev. Lett. **64**, 515 (1990).
[10] L. J. Frasinski, K. Codling, and P. A. Hatherly, Science **246**, 1029 (1989).
[11] J. Ullrich *et al.,* J. Phys. B, At. Mol. Opt. Phys. **30**, 2917 (1997).
[12] R. Moshammer *et al.,* Phys. Rev. Lett. **84**, 447 (2000).
[13] W. Becker, A. Lohr, and M. Kleber, J. Phys. B, At. Mol. Opt. Phys. **27**, L325 (1994).
[14] C. Trump, H. Rottke, and W. Sandner, Phys. Rev. A **60**, 3924 (1999).
[15] K. P. Huber and G. Herzberg, *Molecular Spectra and Molecular Structure, IV. Constants of Diatomic Molecules* (Van Nostrand Reinhold Company, New York, 1979).
[16] M. P. de Boer *et al.,* Phys. Rev. Lett. **71**, 3263 (1993).
[17] J. Ludwig, H. Rottke, and W. Sandner, Phys. Rev. A **56**, 2168 (1997).
[18] D. E. Ramaker and J. M. Peek, At. Data **5**, 167 (1973).
[19] J. H. Posthumus, L. J. Frasinski, A. J. Giles, and K. Codling, J. Phys. B, At. Mol. Opt. Phys. **28**, L349 (1995); T. Seideman, M. Yu. Ivanov, and P. B. Corkum, Phys. Rev. Lett. **75**, 2819 (1995); T. Zuo and A. D. Bandrauk, Phys. Rev. A **52**, R2511 (1995).